AMP-activated protein kinase is a key regulator of retinal vascular permeability

Authors:

Silvia Dragoni[1], Bruna Caridi[1], Eleni Karatsai[1], Mosharraf H. Sarker[1,2], Patric Turowski[1,3]

1. Institute of Ophthalmology, University College London, 11-43 Bath Street, London EC1V 9EL, UK.
2. School of Science, Engineering & Design, Teesside University, Stephenson Street, Middlesbrough TS1 3BA, UK.
3. Corresponding author: p.turowski@ucl.ac.uk

ABSTRACT

Pathological hyperpermeability accompanies many blinding retinopathies. Despite important therapeutic breakthroughs benefitting many but not all retinopathy patients, the intracellular signalling underlying retinal leakage is still poorly understood. We have developed an ex-vivo model, which allowed us to measure and manipulate acute vascular permeability in the intact rodent retina, and combined measurements with immunohistochemical analyses of signal transduction. This ex-vivo retina platform proved to be an easily accessible and reliable tool for systematic identification of regulators of vascular permeability through small molecule antagonists/agonists and siRNA. By using this model, we showed that AMPK was a key mediator of VEGF- and bradykinin-induced permeability by acting downstream of Ca^{2+} and CAMKK, and upstream of eNOS/VE-cadherin as well as p38/HSP27. Accordingly, AMPK agonist potently induced retinal vascular leakage, a finding of major importance for their use as therapeutic agents in the treatment of e.g. cancer or metabolic syndrome.

INTRODUCTION

Leakage within the vascular system is the consequence of endothelial hyperpermeability, which leads to extravasation of fluids and proteins, resulting in interstitial oedema. Vascular leakage can be the cause or a significant co-morbidity of a variety of pathologies, ranging from cancer and inflammation to metabolic diseases such as diabetes[1]. In the nervous system, where the vasculature is uniquely impermeable and is referred to as the blood-brain barrier (BBB), vascular leakage accompanies stroke, multiple sclerosis, as well as various forms of dementia[2]. Leakage at the blood-retinal barrier (BRB) is a hallmark feature of diabetic retinopathy and neovascular age-related macular degeneration[3]. Leakage during diabetic retinopathy, especially diabetic macular oedema is driven by a multitude of extracellular factors including the angiogenic growth factor vascular endothelial growth factor A (VEGF-A) and VEGF-A antagonists are successfully used to reduce oedema and abnormal vessel growth[4]. Despite remarkable efficacy in restoring vision loss in retinal diseases, intraocular anti-VEGF injections only lead to complete resolution of oedema in about half of the patients[5], pointing to the existence of VEGF-independent pathogenic leakage pathways as well as potential resistance to anti-VEGFs. In this regard, current R&D focuses on exploring the therapeutic potential of targeting other permeability-inducing factors relevant to retinal leakage diseases such as angiopoeitin-2[6], lysophosphatidylcholine[7] and bradykinin (BK) [8].

Whilst vascular leakage can be triggered by a wide variety of extracellular molecules, acting on distinct endothelial cell surface receptors, downstream effector mechanisms may be the same to all and ultimately involve paracellular junction modulation or formation of transport vesicles[1,2]. Clearly, endothelial cells regulate hyperpermeability through a core molecular machinery and common, downstream signalling. For

instance, calcium (Ca^{2+}) transients, phosphorylation of the MAP kinase p38 and enhanced actin contractility are associated with all leakage events, as is activation of endothelial nitric oxide synthase (eNOS)[9,10,11,12]. Furthermore, VE-cadherin phosphorylation on tyrosines appears to be a prerequisite for paracellular junction modulation[13]. Identifying such core processes, in particular those with components that are highly specific to vascular beds/leakage, could be desirable for therapeutic development as it would render treatment options independent of specific known (or unknown) extracellular leakage inducers.

In the brain and the retina, entirely different signalling is induced by VEGF-A in endothelial cells when it is added luminally (from the blood side) or abluminally (from the tissue side), with leakage-inducing signalling entirely restricted to abluminal stimulation[10]. For instance, leakage-associated p38 is triggered by abluminal (basal) VEGF-A stimulation, whilst AKT activation, which does not mediate permeability, is only seen following luminal (apical) stimulation. Thus, signalling specific to leakage can be inferred by comparing cellular stimulation following luminal and abluminal addition of VEGF-A. Conversely, BK efficiently induces permeability from the basal as well as apical side of cerebral or retinal endothelial cells.

To identify and validate core components of the leakage machinery in retinal endothelial cells, we adopted an ex vivo retinal preparation, originally described for rats[14]. Development of this method allowed measurement of real time changes of permeability and signalling in intact blood-retinal barrier vessels from rat and mouse. Importantly, this model system was compatible with precise pharmacokinetic agonist studies, parallel IHC staining and manipulation using siRNA. Our workflow can be used to identify core regulators of CNS endothelial hyperpermeability and was validated by identifying the AMP-dependent protein kinase (AMPK) as a novel, key

regulator linking VEGF-A or BK-induced Ca^{2+} transients to eNOS activation and VE-cadherin phosphorylation.

RESULTS

Validation of the ex-vivo retinal model

In order to study VEGF-A-induced permeability in intact retinal microvessels in real time, we adopted an ex-vivo retinal model[14]. Here the method was validated and developed into a discovery and validation platform of core retinal vascular leakage processes.

Immediately after death the head vasculature of rats was perfused and stabilised, and the retinae isolated. Once flatmounted a radial artery was cannulated and the entire retinal vasculature injected with sulforhodamine-B as fluorescent tracer for permeability measurements (Supplementary Figure 1). Subsequently, permeability measurements were carried out by monitoring dye retention continuously by time lapse imaging. A baseline was recorded for at least 30 s, before vasoactive stimulators were added. Permeability (P) values were computed by chosing an area of interest within the dye filled microvessel (Supplemental Figure 2a and b) and by fitting time-dependent pixel intensity changes to the exponential equation $C_t = C_0\ e^{-kt}$, where $k=4P/d$ and d is the diameter of the vessel[10]. Permeability was expressed as changes between pre-treatment and following treatment. For immunohistochemical analysis of permeability associated microvascular changes, flatmounted retinae were stimulated with vasoactive compounds and then fixed at various timepoints.

To assess if the ex vivo preparation and perfusion led to alterations of the retinal vasculature and to determine stability of the preparation, we compared directly

perfused fixed retinae with those perfused with cardioplegic solution and then left under superfusion with Krebs solution for 1 h before fixation. Subsequent whole mount staining for the tight junction protein Claudin-5 (CLDN5) and the adherens junction protein VE-cadherin revealed characteristic strands of continuous paracellular staining (Figure 1a and b) in both preparations. Importantly, the staining pattern was indistinguishable between the two different preparations, indicating that the perfusion did not cause significant disturbances of endothelial junctions. Baseline permeability to sulforhodamine-B was low and on average 0.2 ± 0.16x 10^{-6} cm/s. Taken together these data showed that morphological and barrier properties of the retinal microvasculature were well preserved in these preparations.

Stimulation of the ex-vivo retina with VEGF-A or BK induced similar, ca. 3-fold increases in microvessel permeability (Figures 1c-f). Preincubation of the ex-vivo retina with VEGFR2 inhibitor SU-1498 for 15 min prevented VEGF-A- but not BK-induced permeability, confirming the role of VEGFR2 in VEGF-A-induced permeability and indicating that BK acted through a different receptor. Whole mount retinal staining showed that VEGF-A- and BK-induced permeability coincided with the phosphorylation of p38, its downstream effector HSP27, as well as eNOS (Figure 1g and 1h). Phosphorylation of all three downstream effectors in response to VEGF-A but not BK was abolished following preincubation with SU-1498.

This experimental model was also adapted for mouse retinae (Supplemental Figure 1g). Baseline permeability in mouse preparations was 0.15 ± 0.1x10^{-6} cm/s. VEGF-A stimulation increased permeability to 0.65 ± 0.2x10^{-6} cm/s, and this was again sensitive to SU-1498 (Figure 1i). Furthermore, we observed SU-1498-sensitive phosphorylation of p38, HSP27 and eNOS in mouse retinal microvessels within 2 min of VEGF-A stimulation (Figure 1j). To make the model compatible with knockdown

technology, mouse eyes were injected intravitreously with siRNA against CLDN5. Western blot analysis of retinal lysates, harvested 72 h after the injection, showed that CLDN5 expression was significantly reduced by 65% (Supplemental Figure 2c and d) and this was corroborated by whole mount staining of the retina (Supplemental Figure 2e). Microvessel permeability following knock-down of CLDN5 increased ca. 3-fold (to 0.41±0.03 cm/s) (Supplemental Figure 2f and 2g). Taken together, these results demonstrated that the ex-vivo retinal preparation was a reliable model to measure retinal paracellular microvessel permeability in rats and mice.

VEGF-A and Bradykinin induce AMPK phosphorylation

In order to find new regulators of leakage, primary rat brain ECs were stimulated for 5 or 30 min with VEGF-A (50 ng/ml) from either the apical (non-permeability inducing) or basal (permeability-inducing) side (Figure 2a) and cell lysates analysed by a phospho-protein antibody array. In response to VEGF-A stimulation many signalling components were phosphorylated, as exemplified by p38, HSP27, AMPK, eNOS, SRC, ERK and AKT (Figure 2b and 2c).

Differentially phosphorylated proteins were categorised into three groups; group I phosphorylated only after basal stimulation with VEGF-A (such as p38, HSP27 and AMPK), group II phosphorylated regardless of the side of the stimulation (such as eNOS, SRC and ERK) and group III phosphorylated only when VEGF-A was applied apically (such as AKT). Phosphorylation of proteins exclusively in response to basally applied VEGF-A suggested they played a role in hyperpermeability (group I). Among these, AMPK stood out as it has not been linked to endothelial hyperpermeability before. Additionally, its phosphorylation was also very high in response to basally applied VEGF-A when lysates were analysed by phospho-peptide mass spectrometry

(Dragoni and Turowski, unpublished results). A previous study also suggests that AMPK could link Ca^{2+} transients to VE-cadherin phosphorylation and thus junction opening during pathological signalling in ECs[15].

AMPK phosphorylation in response to VEGF-A was confirmed by Western blot analysis. Stimulation of primary rat brain ECs from the basal side led to rapid, transient phosphorylation of AMPKα, which peaked after ca. 2 min (Figure 2d). A very similar activation pattern was observed in the intact rat retina when VEGF-A was applied directly to the top of the isolated retina (corresponding to the basal side of the endothelium) (Figure 2e).

BK induced similar phosphorylation of AMPKα, both in the cultured primary BMECs and intact retina (Figure 2f and 2g). It was notable that AMPK phosphorylation was maximal after around 2 min in response to both VEGF-A and BK. However, BK clearly induced more sustained phosphorylation.

AMPK mediates VEGF-A/Bradykinin-induced permeability

In order to specify the role of AMPK during VEGF-A- and BK-induced vascular permeability, AMPK activity was neutralised in the ex vivo retina. Preincubation of the ex-vivo retina with compound C, a widely used AMPK antagonist, significantly decreased VEGF-A- and BK- induced permeability by 80% and 93%, respectively (Figure 3a-d). Moreover, whole mount staining showed that pre-treatment with compound C prevented the VEGF-A- and BK-induced activation of p38, HSP27 and eNOS (Figure 3e and f).

Next AMPKα was knocked down specifically by intravitreous injection of siRNA 72 h prior to preparing the retinae for ex vivo permeability measurements. Western blot results showed that AMPKα protein expression was significantly reduced by 70%

(Figures 3g and h). Neither VEGF-A nor BK stimulation resulted in significant permeability in AMPK knocked-down retinae (Figures 3i-l).

Finally, when AMPK was directly activated by treating ex-vivo retinae with A769662 or AICAR, specific AMPK agonists that directly bind to and activate AMPK without any significant change in cellular ATP, ADP or AMP levels, baseline permeability was induced (Figure 4a-d) as well as the phosphorylation of AMPK, p38, HSP27 and eNOS (Figure 4e). Taken together these results confirmed the central role of AMPK in VEGF-A- and BK-induced retinal leakage and showed that AMPK acted upstream of p38 and eNOS.

VEGF-A- and BK-induced permeability requires Ca^{2+} and CaMKK, p38 and eNOS

Next, we aimed at placing AMPK within established permeability signalling cascades. Ca^{2+} is critical for the activation of both p38 and eNOS[15,16,17]. To test its role in VEGF-A-induced vascular leakage the ex-vivo retina was incubated with BAPTA, a Ca^{2+}chelant, prior to VEGF-A administration. BAPTA treatment significantly reduced VEGF-A-induced permeability by 94%, and also prevented the phosphorylation of p38, Hsp27 and eNOS (Figures 5a-c), suggesting that Ca^{2+} acted upstream to these molecules. The Ca^{2+}-dependent CaMKK, is able to phosphorylate and activate AMPK[15,18]. Treatment of retinae with the CaMKK inhibitor STO-609 significantly reduced VEGF-induced permeability by 86% and also prevented the activation of p38, Hsp27 and eNOS (Figure 5d). The role of eNOS in permeability was re-confirmed by preincubation of the ex-vivo retinae with L-NAME, which reduced VEGF-A-induced permeability by 87% but it did not have any effect on p38 or HSP27 phosphorylation (Figure 5e), indicating that eNOS was not upstream of p38. Finally, the ex-vivo retina was preincubated with the p38 inhibitor SB203580. This significantly reduced the

VEGF-A-induced permeability by 80% as well as activation of Hsp27 but not of eNOS (Figure 5f).

Similar results were obtained for BK-induced stimulation of retinae. BAPTA or STO nearly completely abolished BK-induced permeability, together with the activation of p38, Hsp27 and eNOS (Figure 5g-j). Pre-treatment of the ex-vivo retina with L-NAME reduced BK-induced permeability by 67% but did not affect p38 or HSP27 phosphorylation (Figure 5k). Finally, SB203580 prevented BK-induced permeability as well as HSP27 phosphorylation of HSP27 but not eNOS (Figure 5l). Importantly, VEGF-A- or BK-induced phosphorylation of AMPKα was completely abolished by BAPTA or STO. VEGF- but not BK-induced AMPKα phosphorylation was also abolished by SU1498 (Figure 6a).

These results indicated that in the retina VEGF-A and BK induced Ca^{2+} transients and consequent activation of CaMKK and AMPK. At this point signalling diverged into either activation of p38 or eNOS, which both contributed to permeability (Figure 6c).

VEGF-A and BK stimulate VE-Cadherin phosphorylation

Phosphorylation of VE-cadherin is central to paracellular microvascular permeability[13]. VEGF-A or BK stimulation of ex vivo retinae induced tyrosine phosphorylation of VE-cadherin on Y658 in intact microvessels (Figure 6b). This phosphorylation was completely abolished following pre-incubation with compound C, L-NAME but not SB203580, indicating that VE-cadherin was downstream of AMPK/eNOS but not AMPK/p38 (Figure 6c).

DISCUSSION

Measuring retinal microvascular permeability has been mainly restricted to Miles-type assays using either fluorescent tracers or Evans Blue/albumin[7,19]. Chronic leakage can also be visualised in real time by fluorescein angiography[20]. However, collectively these methods, which measure the amount of extravasated tracer, do not only reflect the degree of leakage but are also strongly influenced by dye concentration in the vasculature and dye clearance from the tissue[1,2]. Further disadvantages of these methods are that compound concentrations and timing cannot be controlled accurately. Thus, they are completely inadequate to measure acute permeability and associated signalling.

The ex-vivo retinal platform described herein addressed most of these issues. It constituted a significant advance to endothelial cell cultures, since it used a complete and intact neurovascular unit. The functionality of the retinal vasculature was preserved, with both VE-cadherin and CLDN5 distribution indistinguishable from that in vivo. Similar preparations of the brain and the retina also display full cellular functionality of e.g. pericytes[21]. Importantly, permeability to sulforhodamine-B was very low and within the range of that of the intact BBB in vivo[22] and notably ca. 10 x lower than in preparations of pial micorvessels[23].

Vascular barrier properties in these retinal explants was, as expected dependent on tight junction integrity. The reported speed, at which compounds such as VEGF-A induce permeability[24], was fully recapitulated. Leakage measurements were then combined with whole tissue staining and analyses of the phosphorylation status of key mediators of permeability using phospho-specific antibodies to gain mechanistic insight. Furthermore, the preparations could be interrogated using small molecule antagonists and agonists at defined concentrations and times allowing for the

identification of key downstream regulators, common to VEGF-A and BK stimulation. Even more specific neutralisation of key proteins was achieved through prior intraocular injection of siRNA. Conceivably this model is compatible for use with genetically modified mice and disease models, further broadening its applicability. The ex vivo platform could also be used to measure Ca^{2+} transients or localised production of reactive oxygen or nitrogen species in response to vasoactive compounds such as VEGF or BK.

Measurements in retinae were done ex vivo, in the absence of blood flow. Blood flow and associated shear stress may influence endothelial cell biology, such as cell-cell adhesion and inflammatory dysfunction[13,25,26] and their absence in our preparation must be taken into account when evaluating results. However, it should also be noted that permeability regulation by shear stress appears to be remembered in ECs in vitro for at least 24 h[27].

For the purpose of developing and validating the ex vivo retinal platform we have focused on permeability factors, which induce permeability when added to the abluminal (tissue) side of the endothelium, such as VEGF-A and BK[10], as these are readily applied on top of the retinal explants. Other permeability factors that act only from the luminal side, such as lysophosphatidic acid[10] or lysophosphatidylcholine[7], could also potentially be investigated in this system. However, this would require the use of a manifold injection system[28], which allows switching between injection of sulforhodamine-B with or without permeability factor into radial vessels.

VEGF-A and BK induced acute leakage in retinal microvessels, which was associated with and dependent on Ca^{2+}, the MAPK p38 and eNOS, in agreement with published data[9,10,12]. We also identified AMPK as a novel, key regulator of both VEGF-A- and BK-induced permeability, indicating it is a core regulator of vascular permeability. This

protein kinase is primarily known to regulate energy requirements of the cell, but has also been implicated in other seemingly unrelated cellular processes such as migration, cell growth and apoptosis[29], but crucially not yet in endothelial permeability. Whilst its canonical activation is dependent on cellular AMP: ATP concentrations and phosphorylation on T172 by LKB1, we found that, in the regulation of endothelial permeability, AMPK was activated downstream of Ca^{2+} and CaMKKβ. This activation pathway has previously been described as non-canonical[30] and is also operational when CNS endothelial cells facilitate the transmigration of lypmphocytes[15]. Notably, VEGF-A has been reported before to induce NO production via a pathway requiring Ca^{2+} and AMPK[31]. Indeed, eNOS phosphorylation on S1179 can be mediated by AKT[32] or AMPK[15,33]. However, AKT activity is not relevant to permeability induction in neurovascular endothelial cells, as it is not activated in response to permeability-inducing (abluminal) VEGF-A stimulation[10]. We confirmed the phosphorylation of eNOS on S1179 downstream of AMPK both in response to VEGF-A and BK stimulation and its requirement for successful permeability induction. Interestingly, the Ca^{2+}/AMPK/eNOS pathway resulted in the phosphorylation of VE-cadherin on Y658, identified previously as important for vascular permeability[13], thus providing a direct link between AMPK and paracellular junction regulation.

During retinal permeability, AMPK also regulated the phosphorylation of the MAPK p38 and its substrate HSP27. P38 is a bona fide regulator of VEGF-A responses[34] and its activation downstream of cdc42 and PAK and subsequent modulation of the actin cytoskeleton occurs during VEGF-induced endothelial migration downstream of VEGFR2 phosphorylation on Y1214[35]. Whilst it is possible that additional, parallel AMPK regulation of this cascade was operational during VEGF-A or BK-induced permeability, we favour an alternative model of direct activation of p38 by AMPK via

TAB1, a pathway described in apoptotic lymphocytes and the ischemic heart[36,37]. By switching between two different p38 activation modes (Ca^{2+}/AMPK/TAB1 versus cdc42/PAK) endothelial cells could adapt cytoskeletal regulation to the specific requirement of endothelial cell migration or permeability.

The reliable permeability and signalling measurement of ex vivo retina platform provides all the necessary requirements to identify novel key mediators of vascular leakage and test their druggability. Whilst AMPK clearly emerged as such a key regulator, it is unlikely to be exploitable as a target for anti-leakage treatments: its central role in regulating cellular energy demands throughout the body hints at many potential side effects. Activation of AMPK is currently investigated as a therapeutic option to treat cancer, metabolic syndrome and diabetes[38,39]. However, in light of the strong induction of permeability we observed in response to at least two AMPK agonists, we propose that these avenues should be explored cautiously, since microvascular leakage may accompany such treatment modalities. Nevertheless, this discovery indicated that the ex vivo retina platform can play an important part in future discoveries of anti-leakage drug targets.

ACKNOWLEDGEMENTS

We thank Dr Paul Fraser (King's College London) for introducing us to early ex-vivo retinal preparation and Prof. John Greenwood (UCL) for critical comments on the manuscript. siRNAs targeting CLDN5 were kindly provided by Dr Matthew Campbell (Trinity College Dublin). This work was supported by a Moorfields Eye Charity grant to S.D. and a Diabetes UK grant to P.T.

The data that support the findings of this study are available from the corresponding author upon reasonable request.

MATERIALS AND METHODS

Materials

Recombinant rat VEGF-A(165) was purchased from R&D Systems (Abingdon, United Kingdom). Bradykinin, Sulforhodamine-B, Evans blue, SU-1498, SB-203580, Compound-C, STO-609, L-NAME, BAPTA-AM, AICAR and A769662 were purchased from MERCK (Dorset, United Kingdom).

Polyclonal antibodies specific for p38, Hsp27, AMPKα, eNOS and their phosphorylated forms (p38 Thr180/Tyr182, pHSP27 Ser82, AMPK Thr172 and eNOS Ser1177) were from Cell Signaling Technology (Beverly, MA).

Solutions

Heparinized saline: 300U/L heparin in 0.9% NaCl.

Cardioplegic solution: 10 mM Mg2+, 110 mM NaCl, 8 mMKCl, 10 mM HEPES, 1 mM CaCl2, pH 7.0. 10 µM Isoproterenol to be added before use.

Evans Blue dye: 5.0 g/L Evans Blue dye in cardioplegic solution supplemented with 10% albumin.

Krebs solution: 124 mM sodium chloride, 5 mM potassium chloride, 2 mM MgSO4, 0.125 mM NaH2 PO4, 22 mM NaHCO3, 2 mM CaCl2, pH 7.4. 5 mM glucose and 0.1% BSA to be added before use.

Sulforhodamine-B solution: 1mg/ml Sulforhodamine-B in Krebs solution.

Blocking buffer: 3% Triton X-100, 1% Tween, 0.5% Bovine Serum Albumin in 2x PBS

Animals

Wistar female rats and C75BL/6J mice were purchased from Charles River Laboratories. All procedures were performed with accordance with the UK Animals Act and with the Association for Research in Vision and Ophthalmology Statement for the Use of Animals in Ophthalmic and Vision Research and the Animal Welfare and the Ethical Review Bodies of the UCL Institute of Ophthalmology.

Methods

Retinal explant preparation

Wistar female rats were killed by overdose of CO_2. Rats were placed in a lateral decubitus position under the dissection microscope and were securely maintained with tape. The skin of the neck region was gently cut off and an incision of approximately 15 mm over the thyroid bone exposed the salivary glands which were gently pushed sideways, uncovering the neighbouring muscles. Lateral traction of the aforementioned muscles enabled visual access to the common carotid artery. Then the common carotid artery was carefully exposed, elevated and separated from the vagus nerve using forceps and a 7-0 suture which was initially placed below the artery and later used to tie securely a microcannula after its insertion. A small cut was performed to the distal part of the common carotid artery through which a microcannula was inserted and further advanced along the artery's length for approximately 5 mm. Flow-back of blood into the tip of the cannula provided evidence of the cannula being in situ. Then a tie was used to maintain the steadiness of the cannulated structure and a flush of heparinized saline was introduced into the vasculature by a 10 ml syringe. This initial flush was followed by a second flush of

stabilizing solution, also referred to as cardioplegic solution containing isoproterenol and subsequently, Evans blue dye. The introduction of Evans Blue in the common carotid artery induced immediate visualization of the blue dye circulation on the ipsilateral part of the head and neck of the animal.

Next, the eyes were surgically removed and placed in PBS. One eye was enucleated, and the retina was isolated, together with the attached sclera. The retina was flattened onto a transparent silicone medium (SYLGARD® 184 SILICONE ELASTOMER KIT by Dow Corning) and kept in position by a metal ring, placed on the top and pinned to the silicon pad with metal pins. The ring was surrounded by grease and the retina was continuously superfused with Krebs solution .

Needle preparation

Glass capillary needles were made using standard wall borosilicate tubing with filament (outer diameter: 1.00mm, inner diameter: 0.50mm and length: 10cm) and a needle puller (Fleming/Brown Micropipette Puller P-97), with a 3.0 mm square box filament 3.0 mm wide (Sutter Instrument Company). Parameters were set to temperature: 580, pressure: 300, velocity 50, time 80. Tips of the needles were bevelled at a 20º on an EG-400 Micro Grinder (Narishige), resulting in very sharp tips. The needle was placed into a needle holder, connected to a syringe and mounted on a Leitz micromanipulator.

Permeability measurements

Experiments and image acquision were carried out using a platform that was built from a Zeiss Axiophot fluorescent microscope. This set-up includes: a Leica EL6000 lamp that uses an alignment-free, mercury metal halide bulb and has an integrated fast

shutter; a Hamamatsu digital camera and camera controller, a mobile stage that we built under the objectives, on the top of which we put a plastic cylinder, customised to hold in place the silicon pad on which we flattened the retina.

The retina was visualised using Zeiss ACHROPLAN 10X/0.25 objective, working distance 6.0 mm. Microinjection needles were front filled with a 0.22 µm filtered solution of sulforhodamine B (1 mg/ml in Krebs solution). The needle was used to cannulate a radial vessel from above, approximately 150 µm far from the optic nerve and sulforhodamine-B was injected by increasing the pressure in the needle through the syringe. The needle was kept at an angle of ca. 20º to avoid crossing and puncturing the vessel on both sides.

Successful cannulation of the radial vessel was indicated by the vasculature turning pink, at which time illumination was switched to fluorescence and the vessels were visualized under a TRITC filter using a Olympus LUMPLFL 40X/0.80 water immersion objective, working distance 3.3 mm. A microvessel was chosen at least 200 µm away from the cannulated radial vessel and then continuously visualized through the digital camera on a computer screen. The fluorescent vessel was recorded continuously by time lapse (1 frame/2 s) imaging for at least 2 min. A baseline was recorded for at least 30 s, before VEGF-A or BK in Krebs solution was added on the top of the retina under continuous recording.

Data were extrapolated using ImageJ. A measurement square box was drawn inside of a chosen vessel, box size was approximately 18 x 18 pixels, depending on the size of the vessel. Background was measured and subtracted from the fluorescence measurements. Pixel intensity measurements were charted against time, and permeability values were computed by fitting data to the exponential equation Ct = C0 e-kt, where k=4P/d and d is the diameter of the vessel[10]. Effects were measured as

permeability changes between pre-treatment baseline and following treatment (Figure 1f).

Primary rat brain EC Isolation

Microvessels were isolated from rat cortical gray matter by collagenase dispase digestion and BSA and Percoll density gradient centrifugation[10]. Purified vessels were seeded onto collagen IV/fibronectin-coated Costar Transwells (Fisher Scientific) at high density (vessels from 6 rat brains per 40 cm^2). Cells were grown in EGM2-MV (Lonza), with 5 mg/ml puromycin from the second day for 3 days, for 2–3 weeks until their TEER plateaued at values above 200 Ω.cm2.

Phosphoantibody array

Mature monolayers of primary, unpassaged BMVECs grown on 24 mm Costar Transwells were stimulated with VEGF-A (50 ng/ml) from the apical or basal side for 5 or 30 min. Cells from 2 Transwells were combined by lysis in 200 µL of lysis buffer and subjected to screening using Human Phospho-Kinase Array Proteome Profiler Array (R&D Systems; ARY003B) exactly according to the manufacturer's instructions. Arrays were exposed for varying amounts of time to capture signals in the linear range and quantified by densitometric scanning and ImageJ (NIH). Signals were normalised using array-internal controls. Results were expressed as fold-differences between apical versus basal signals.

Western Blots

Cell lysates were prepared as previously described[10]. Proteins were separated by SDS-PAGE and transferred to nitrocellulose by semidry electrotransfer. Membranes

were blocked o/n and then incubated with the appropriate antibody diluted at 1:2,000. Membranes were washed three times with TBS/0.1% Tween-20 before 1h incubation with an anti-mouse or anti-rabbit HRP-conjugated IgG (GE Healthcare) at a dilution of 1:10,000 and 1:5,000, respectively. Membranes were developed using the ECL reagents (Roche) and exposed to X-ray film. Protein bands were evaluated by densitometric quantification, normalized against the amount of total protein, and GADPH or Tubulin.

Immunohistochemistry

After dissection, retinae from rat or mouse were fixed with 4% PFA at room temperature for 1h. After 30 min of blocking, retinae were incubated with primary antibodies against Isolectin B4 (IB-4), P-p38, P-HSP27, P-eNOS, P-AMPKα, CLDN5and P-VE-Cadherin at 4 ºC o/n. Retinae were washed and incubated with matching Alexa Fluor conjugated secondary antibodies at room temperature for 2 h. Finally, retinae were washed and mounted using Mowiol 4-88 mounting medium (Sigma). (refer to ref 9 for more details).

siRNA-mediated Knockdown of Claudin-5 and AMPKα

Specific SiRNA sequences targeting Caludin-5 or the α subunit of AMPK were purchased from Dharmacon (Chicago, IL). Mice were anesthetised by intraperitoneal injection of 100 ul of 6% Narketan (ketamine) and 10% Dormitor (medetomidine) in sterile water. 2 µl of the siRNA (1ng/ml in sterile PBS) were injected intravitreously in the right eye under a stereomicroscope, using a Hamilton syringe with a 3 degrees Hamilton RN needle (Esslab). Two microliters of sterile PBS were injected into the left eye as a control. To inject, an initial puncture was made to the superior nasal sclera,

at the level of the pars plana. Then, the tip of the needle was further introduced through the puncture hole with a 45-degree angle into the vitreous body. Retinae were isolated 72 h after the injection.

Statistics

Densitometric quantification of four independent immunoblots were determined by changes in phosphoprotein content normalized to tubulin or GADPH/total protein loading controls, with values expressed as fold increase. Data were presented as mean ± SEM. Statistics were performed using one-way ANOVA with significance levels set at 0.05, followed by Student t test (for pairwise comparison), * $p < 0.05$; **, $0.001 < p < 0.01$, ***, $p \leq 0.001$.

REFERENCES

1 Nagy, J. A., Benjamin, L., Zeng, H., Dvorak, A. M. & Dvorak, H. F. Vascular permeability, vascular hyperpermeability and angiogenesis. *Angiogenesis* **11**, 109-119, doi:10.1007/s10456-008-9099-z (2008).

2 Turowski, P. in *The Blood Brain Barrier and Inflammation.* (ed Springer Link) 81-102 (2017).

3 Klaassen, I., Van Noorden, C. J. & Schlingemann, R. O. Molecular basis of the inner blood-retinal barrier and its breakdown in diabetic macular edema and other pathological conditions. *Prog Retin Eye Res* **34**, 19-48, doi:10.1016/j.preteyeres.2013.02.001 (2013).

4 Brown, D. M. *et al.* Long-term outcomes of ranibizumab therapy for diabetic macular edema: the 36-month results from two phase III trials: RISE and RIDE. *Ophthalmology* **120**, 2013-2022, doi:10.1016/j.ophtha.2013.02.034 (2013).

5 Ford, J. A. *et al.* Current treatments in diabetic macular oedema: systematic review and meta-analysis. *BMJ Open* **3**, doi:10.1136/bmjopen-2012-002269 (2013).

6 Campochiaro, P. A. & Peters, K. G. Targeting Tie2 for Treatment of Diabetic Retinopathy and Diabetic Macular Edema. *Curr Diab Rep* **16**, 126, doi:10.1007/s11892-016-0816-5 (2016).

7 Canning, P. *et al.* Lipoprotein-associated phospholipase A2 (Lp-PLA2) as a therapeutic target to prevent retinal vasopermeability during diabetes. *Proc Natl Acad Sci U S A* **113**, 7213-7218, doi:10.1073/pnas.1514213113 (2016).

8 Kita, T. *et al.* Plasma Kallikrein-Kinin System as a VEGF-Independent Mediator of Diabetic Macular Edema. *Diabetes* **64**, 3588-3599, doi:10.2337/db15-0317 (2015).

9 Wu, H. M., Yuan, Y., Zawieja, D. C., Tinsley, J. & Granger, H. J. Role of phospholipase C, protein kinase C, and calcium in VEGF-induced venular hyperpermeability. *Am J Physiol* **276**, H535-542, doi:10.1152/ajpheart.1999.276.2.H535 (1999).

10 Hudson, N. *et al.* Differential apicobasal VEGF signaling at vascular blood-neural barriers. *Dev Cell* **30**, 541-552, doi:10.1016/j.devcel.2014.06.027 (2014).

11 Weidert, E., Pohler, S. E., Gomez, E. W. & Dong, C. Actinomyosin contraction, phosphorylation of VE-cadherin, and actin remodeling enable melanoma-induced endothelial cell-cell junction disassembly. *PLoS One* **9**, e108092, doi:10.1371/journal.pone.0108092 (2014).

12 Di Lorenzo, A. *et al.* eNOS-derived nitric oxide regulates endothelial barrier function through VE-cadherin and Rho GTPases. *J Cell Sci* **126**, 5541-5552, doi:10.1242/jcs.115972 (2013).

13 Orsenigo, F. *et al.* Phosphorylation of VE-cadherin is modulated by haemodynamic forces and contributes to the regulation of vascular permeability in vivo. *Nat Commun* **3**, 1208, doi:10.1038/ncomms2199 (2012).

14 Warboys, C. M., Toh, H. B. & Fraser, P. A. Role of NADPH oxidase in retinal microvascular permeability increase by RAGE activation. *Invest Ophthalmol Vis Sci* **50**, 1319-1328, doi:10.1167/iovs.08-2730 (2009).

15 Martinelli, R. *et al.* ICAM-1-mediated endothelial nitric oxide synthase activation via calcium and AMP-activated protein kinase is required for transendothelial lymphocyte migration. *Mol Biol Cell* **20**, 995-1005, doi:10.1091/mbc.E08-06-0636 (2009).

16 Takeda, K. *et al.* Involvement of ASK1 in Ca2+-induced p38 MAP kinase activation. *EMBO Rep* **5**, 161-166, doi:10.1038/sj.embor.7400072 (2004).

17 da Silva, C. G., Specht, A., Wegiel, B., Ferran, C. & Kaczmarek, E. Mechanism of purinergic activation of endothelial nitric oxide synthase in endothelial cells. *Circulation* **119**, 871-879, doi:10.1161/CIRCULATIONAHA.108.764571 (2009).

18 Hurley, R. L. *et al.* The Ca2+/calmodulin-dependent protein kinase kinases are AMP-activated protein kinase kinases. *J Biol Chem* **280**, 29060-29066, doi:10.1074/jbc.M503824200 (2005).

19 Radu, M. & Chernoff, J. An in vivo assay to test blood vessel permeability. *J Vis Exp*, e50062, doi:10.3791/50062 (2013).

20 Couturier, A. *et al.* Widefield OCT-Angiography and Fluorescein Angiography Assessments of Nonperfusion in Diabetic Retinopathy and Edema Treated with Anti-Vascular Endothelial Growth Factor. *Ophthalmology*, doi:10.1016/j.ophtha.2019.06.022 (2019).

21 Mishra, A. *et al.* Imaging pericytes and capillary diameter in brain slices and isolated retinae. *Nat Protoc* **9**, 323-336, doi:10.1038/nprot.2014.019 (2014).

22 Smith, Q. R. & Rapoport, S. I. Cerebrovascular permeability coefficients to sodium, potassium, and chloride. *J Neurochem* **46**, 1732-1742, doi:10.1111/j.1471-4159.1986.tb08491.x (1986).

23 Easton, A. S., Sarker, M. H. & Fraser, P. A. Two components of blood-brain barrier disruption in the rat. *J Physiol* **503 (Pt 3)**, 613-623, doi:10.1111/j.1469-7793.1997.613bg.x (1997).

24 Bates, D. O. Vascular endothelial growth factors and vascular permeability. *Cardiovasc Res* **87**, 262-271, doi:10.1093/cvr/cvq105 (2010).

25 Chistiakov, D. A., Orekhov, A. N. & Bobryshev, Y. V. Effects of shear stress on endothelial cells: go with the flow. *Acta Physiol (Oxf)* **219**, 382-408, doi:10.1111/apha.12725 (2017).

26 Ho, R. X. *et al.* The cell adhesion molecule IGPR-1 is activated by, and regulates responses of endothelial cells to shear stress. *J Biol Chem*, doi:10.1074/jbc.RA119.008548 (2019).

27 Walsh, T. G. *et al.* Stabilization of brain microvascular endothelial barrier function by shear stress involves VE-cadherin signaling leading to modulation of pTyr-occludin levels. *J Cell Physiol* **226**, 3053-3063, doi:10.1002/jcp.22655 (2011).

28 Liu, B., Shao, Y. & Mirkin, M. V. Dual-pipet techniques for probing ionic reactions. *Anal Chem* **72**, 510-519, doi:10.1021/ac990771p (2000).

29 Hardie, D. G. AMP-activated protein kinase: an energy sensor that regulates all aspects of cell function. *Genes Dev* **25**, 1895-1908, doi:10.1101/gad.17420111 (2011).

30 Carling, D., Sanders, M. J. & Woods, A. The regulation of AMP-activated protein kinase by upstream kinases. *Int J Obes (Lond)* **32 Suppl 4**, S55-59, doi:10.1038/ijo.2008.124 (2008).

31 Reihill, J. A., Ewart, M. A., Hardie, D. G. & Salt, I. P. AMP-activated protein kinase mediates VEGF-stimulated endothelial NO production. *Biochem Biophys Res Commun* **354**, 1084-1088, doi:10.1016/j.bbrc.2007.01.110 (2007).

32 Fulton, D. *et al.* Regulation of endothelium-derived nitric oxide production by the protein kinase Akt. *Nature* **399**, 597-601, doi:10.1038/21218 (1999).

33 Youn, J. Y., Wang, T. & Cai, H. An ezrin/calpain/PI3K/AMPK/eNOSs1179 signaling cascade mediating VEGF-dependent endothelial nitric oxide production. *Circ Res* **104**, 50-59, doi:10.1161/CIRCRESAHA.108.178467 (2009).

34 Corre, I., Paris, F. & Huot, J. The p38 pathway, a major pleiotropic cascade that transduces stress and metastatic signals in endothelial cells. *Oncotarget* **8**, 55684-55714, doi:10.18632/oncotarget.18264 (2017).

35 Lamalice, L., Houle, F., Jourdan, G. & Huot, J. Phosphorylation of tyrosine 1214 on VEGFR2 is required for VEGF-induced activation of Cdc42 upstream of SAPK2/p38. *Oncogene* **23**, 434-445, doi:10.1038/sj.onc.1207034 (2004).

36 Li, J., Miller, E. J., Ninomiya-Tsuji, J., Russell, R. R., 3rd & Young, L. H. AMP-activated protein kinase activates p38 mitogen-activated protein kinase by increasing recruitment of p38 MAPK to TAB1 in the ischemic heart. *Circ Res* **97**, 872-879, doi:10.1161/01.RES.0000187458.77026.10 (2005).

37 Lanna, A., Henson, S. M., Escors, D. & Akbar, A. N. The kinase p38 activated by the metabolic regulator AMPK and scaffold TAB1 drives the senescence of human T cells. *Nat Immunol* **15**, 965-972, doi:10.1038/ni.2981 (2014).

38 Hardie, D. G. Targeting an energy sensor to treat diabetes. *Science* **357**, 455-456, doi:10.1126/science.aao1913 (2017).

39 Kim, J., Yang, G., Kim, Y., Kim, J. & Ha, J. AMPK activators: mechanisms of action and physiological activities. *Exp Mol Med* **48**, e224, doi:10.1038/emm.2016.16 (2016).

FIGURE LEGENDS

Figure 1. Validation of the ex vivo retina model in rats. (a-b) Control retinae were from animals directly perfused fixed with 4% PFA. Ex vivo retinae were isolated as described, flat mounted and left submerged with Krebs solutions for 1h before PFA fixation. Whole mounts were stained for Isolectin B4 (IB4, green), CLDN5 (magenta) and VE-cad (magenta) as indicated. **(c-f)** Sulforhodamine-B fluorescent intensities were recorded in single retinal capillaries. 50 ng/ml VEGF-A (c-d) or 10uM Bradykinin (BK) (e-f) were applied on top of the retina (abluminal side) at times indicated. Optionally retinae were preincubated with the VEGFR2-selective antagonist SU1498 (10 µM) for 15 min prior to recording. Permeability changes assembled from at least four retinae are shown in (d) and (f). **(g-h)** Ex-vivo retinal explants were incubated with with VEGF-A (g) or BK (h) for 2 min, fixed using 4% PFA and then stained for phospho-p38, phospho-Hsp27 or phospho-eNOS. **(i)** Mouse retinae were preincubated with or without SU1498 (10 µM) for 15 minutes. VEGF-A was then applied to the top of the retina and changes in fluorescence were recorded. **(j)** Mouse retinal explants were stimulated and stained as described in panel (g) using phosphor-specific antibodies to p38, HSP27 and eNOS. *$p < 0.05$, **$p < 0.01$, ***$p < 0.001$. Scale bars, 10 µm.

Figure 2. VEGF-A and Bradykinin induced AMPK phosphorylation. (a-c) Primary brain microvascular ECs (BMECs) were stimulated with VEGF-A from the apical or basal side for 5 min triggering apically (group I), basally specific (group III) or mixed (group II) responses (see text or ref 9 for more details)(a). Cells were lysed and phosphorylation of indicated molecules assessed by phosphoantibody array analysis (b-c). **(d-g)** BMECs (d, f) or ex-vivo rat retinae (e, g) were stimulated with 50 ng/ml

VEGF-A (d-e) or 10 μM BK (f-g) for the indicated length of time and AMPKα phosphorylation analysed. Representative results and quantification of AMPKα activation from three independent experiments are shown. *$p < 0.05$, **$p < 0.01$, ***$p < 0.001$.

Figure 3. AMPK mediated VEGF-A/Bradykinin-induced permeability. (a-f) Mouse ex-vivo retinae were preincubated with or without Compound-C (10 μM) for 15 minutes. 10 ng/ml VEGF-A (a) or 10 μM BK (b) were then applied to the top of the retina and changes in fluorescence were recorded (c, d) or phosphorylation of p38, HSP27 and eNOS was assessed by staining (e, f). (g-l) AMPKα was knocked down by intravitreous injection of a specific siRNA (g, h) and ex-vivo retinae were isolated after at least 48h. VEGF-A (50 ng/ml) (I, k) or BK (10 μM) (j, l) did not induce any permeability in the knocked down ex-vivo retina. Representative results and quantifications (normalized mean ± SEM) from three independent experiments are shown. *$p < 0.05$, **$p < 0.01$, ***$p < 0.001$. Scale bars, 10 μm.

Figure 4. Stimulation of AMPK induced permeability in the ex-vivo retina. (a-e) Ex-vivo preparations were stimulated with two different AMPK activators named A769662 (10 μM) and AICAR (10 μM). Both agonists induced permeability in the ex-vivo retina (a-d) together with the activation of p38, HSP27 and eNOS (e). Permeability changes assembled from at least four retinae are shown.*$p < 0.05$, **$p < 0.01$, ***$p < 0.001$. Scale bars, 10 μm.

Figure 5. VEGF-A- and Bradykinin-induced permeability requires Ca^{2+} and activation of CaMKK, p38 and eNOS. **(a-l)** Ex-vivo retinae were preincubated with 20 µM BAPTA (Ca^{2+}chelator) (c, i), or 10uM STO (CaMKK inhibitor) (d, j), or 10 µM L-NAME (eNOSinhibitor) (e, k) or 10 µM SB202190 (SB) (p38 inhibitor) (f, l), for 15 minutes and VEGF-A (50 ng/ml) or BK (10 µM) were then applied to the top of the retina (abluminal side) and changes in fluorescence were recorded or phosphorylation of p38, HSP27 and eNOS was assessed by staining. VEGF-A and BK-induced permeability was mediated by Ca^{2+}, CaMKK, eNOS and p38. Representative results and quantifications (normalized mean ± SEM) from four independent experiments are shown. *$p < 0.05$, **$p < 0.01$, ***$p < 0.001$. Scale bars, 10 µm.

Figure 6. VEGF-A and Bradykinin induced VE-Cadherin phosphorylation

(a) Ex-vivo retinae were preincubated with SU1498 (10 µM), or BAPTA (20 µM) or STO (10 µM) and treated with VEGF-A and Brdykinin for 2 min. Retinae were then fixed with 4% PFA and whole mount stained for phospho-AMPKα (magenta) against IB4 (green). **(b)** Ex-vivo retinae were preincubated with compound C (10 µM), or L-NAME (10 µM) or SB202190 (10 µM), treated with VEGF-A and Bradykinin for 2 min and whole mount stained for phospho-VE-Cadherin (magenta) against IB4 (green). **(c)** Proposed signaling networks in the ex-vivo retinal microvasculature downstream of VEGF-A and Bradykinin. Scale bars, 10 µm.

Supplemental Figure 1. The ex-vivo retinal model. (a-b) The carotid artery of a rat was separated from the surrounding tissues, cannulated using a microcannula (a) and consecutively perfused with heparin, cardioplegic solution without and with Evans Blue (b). **(c-d)** The retina was isolated together with the sclera and flat-mounted onto a

transparent silicon medium using a metal ring and pins (c). The retinal microvasculature was filled with Sulforhodamine-B through injection of a radial vessel using a sharpened glass capillary needle (d). **(e-f)** A capillary was chosen at least 200 µm away from the injection site (e) and the baseline fluorescence intensity within the vessel recorded for ca. 30 s before VEGF-A or BK were applied on top of the retina and permeability determined from time-dependent loss of fluorescence (f) Scale bar, 20 µm. **(g)** Differences between the retinal vasculature and set-up in rats and mice. Shown are images of retinal microvessels, the metal mounting ring and the microinjection needles.

Supplemental Figure 2. Properties of the ex-vivo retina model. (a-b) Selected frames, pseudocoloured in (b), of timelapse measurement of a sulforhodamine-filled rat capillary before and after the addition of 50 ng/ml VEGF-A, illustrating the rapid loss of fluorophore from the lumen of the vessel. The red box indicates the r.o.i for intensity measurement. Scale bars, 10 µm. **(c-f)** CLDN5 siRNA was injected into mouse eyes. 48 h later CLDN5 levels were analysed by immunoblots of retinal lysates (c-d) or by wholemount immunochemical staining (e). Scale bar, 100 µm. Alternatively, permeability of 4 KDa Rhodamine was measured in ex vivo retinae from CLDN5 siRNA treated or control eyes (f-g). *$p < 0.05$, **$p < 0.01$, ***$p < 0.001$.

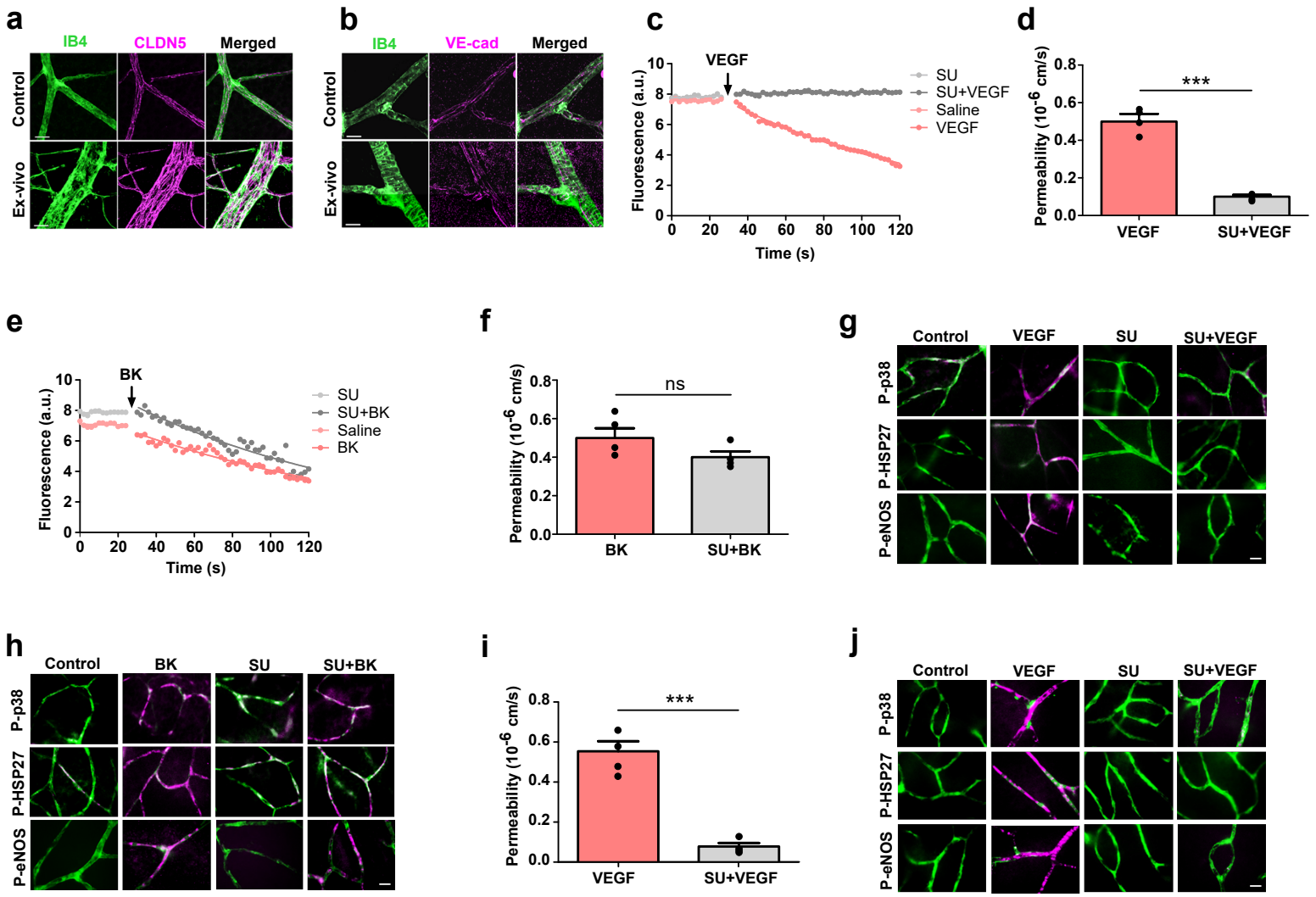

Figure 1. Validation of the ex vivo retina model in rats. (a-b) Control retinae were from animals directly perfused fixed with 4% PFA. Ex vivo retinae were isolated as described, flat mounted and left submerged with Krebs solutions for 1h before PFA fixation. Whole mounts were stained for Isolectin B4 (IB4, green), CLDN5 (magenta) and VE-cad (magenta) as indicated. **(c-f)** Sulforhodamine-B fluorescent intensities were recorded in single retinal capillaries. 50 ng/ml VEGF-A (c-d) or 10uM Bradykinin (BK) (e-f) were applied on top of the retina (abluminal side) at times indicated. Optionally retinae were preincubated with the VEGFR2-selective antagonist SU1498 (10 μM) for 15 min prior to recording. Permeability changes assembled from at least four retinae are shown in (d) and (f). **(g-h)** Ex-vivo retinal explants were incubated with with VEGF-A (g) or BK (h) for 2 min, fixed using 4% PFA and then stained for phospho-p38, phospho-Hsp27 or phospho-eNOS. **(i)** Mouse retinae were preincubated with or without SU1498 (10 μM) for 15 minutes. VEGF-A was then applied to the top of the retina and changes in fluorescence were recorded. **(j)** Mouse retinal explants were stimulated and stained as described in panel (g) using phosphor-specific antibodies to p38, HSP27 and eNOS. *$p < 0.05$, **$p < 0.01$, ***$p < 0.001$. Scale bars, 10 μm.

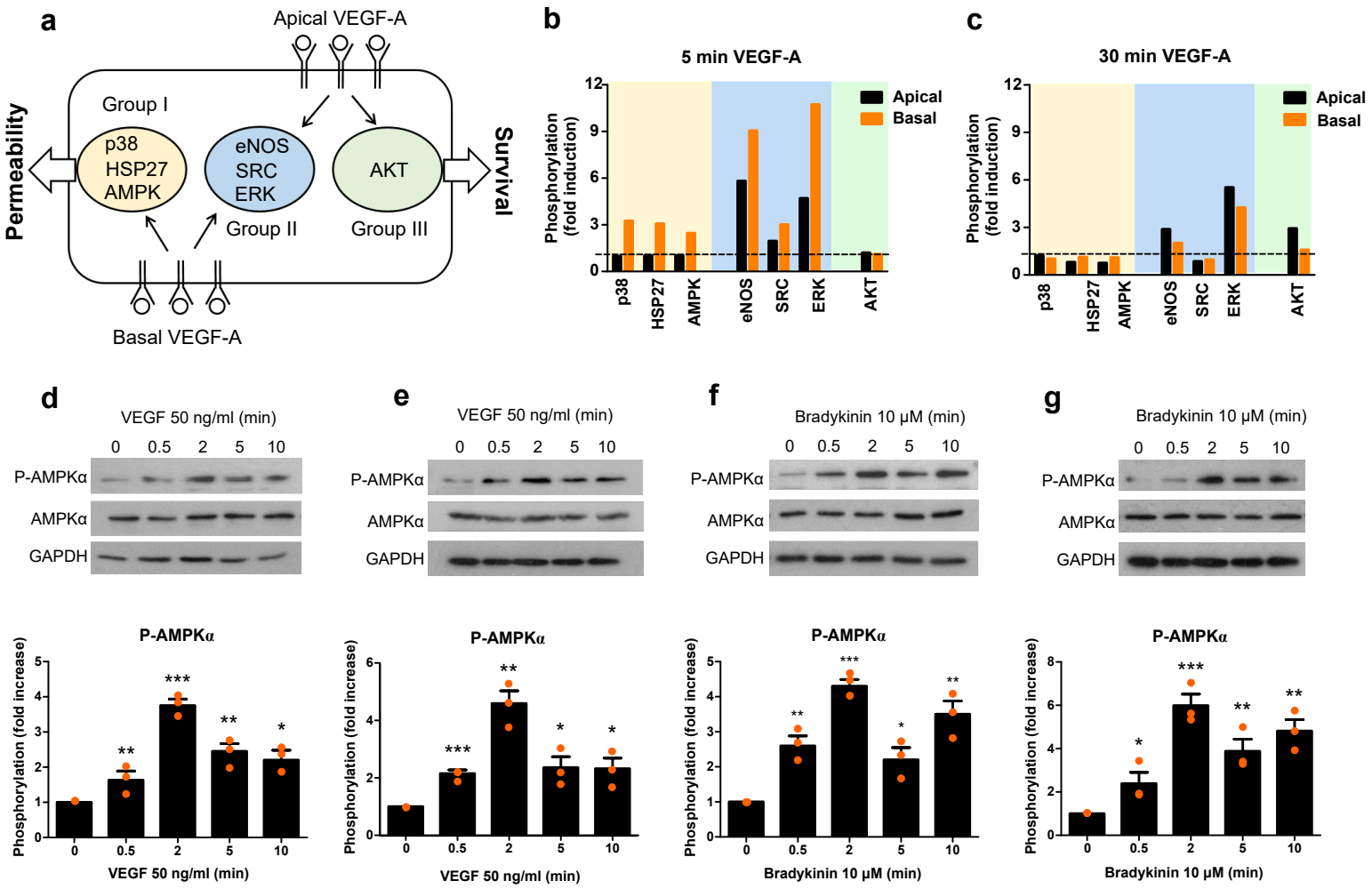

Figure 2. VEGF-A and Bradykinin induced AMPK phosphorylation. (a-c) Primary brain microvascular ECs (BMECs) were stimulated with VEGF-A from the apical or basal side for 5 min triggering apically (group I), basally specific (group III) or mixed (group II) responses (see text or ref 9 for more details)(a). Cells were lysed and phosphorylation of indicated molecules assessed by phosphoantibody array analysis (b-c). **(d-g)** BMECs (d, f) or ex-vivo rat retinae (e, g) were stimulated with 50 ng/ml VEGF-A (d-e) or 10 μM BK (f-g) for the indicated length of time and AMPKα phosphorylation analysed. Representative results and quantification of AMPKα activation from three independent experiments are shown. *$p < 0.05$, **$p < 0.01$, ***$p < 0.001$.

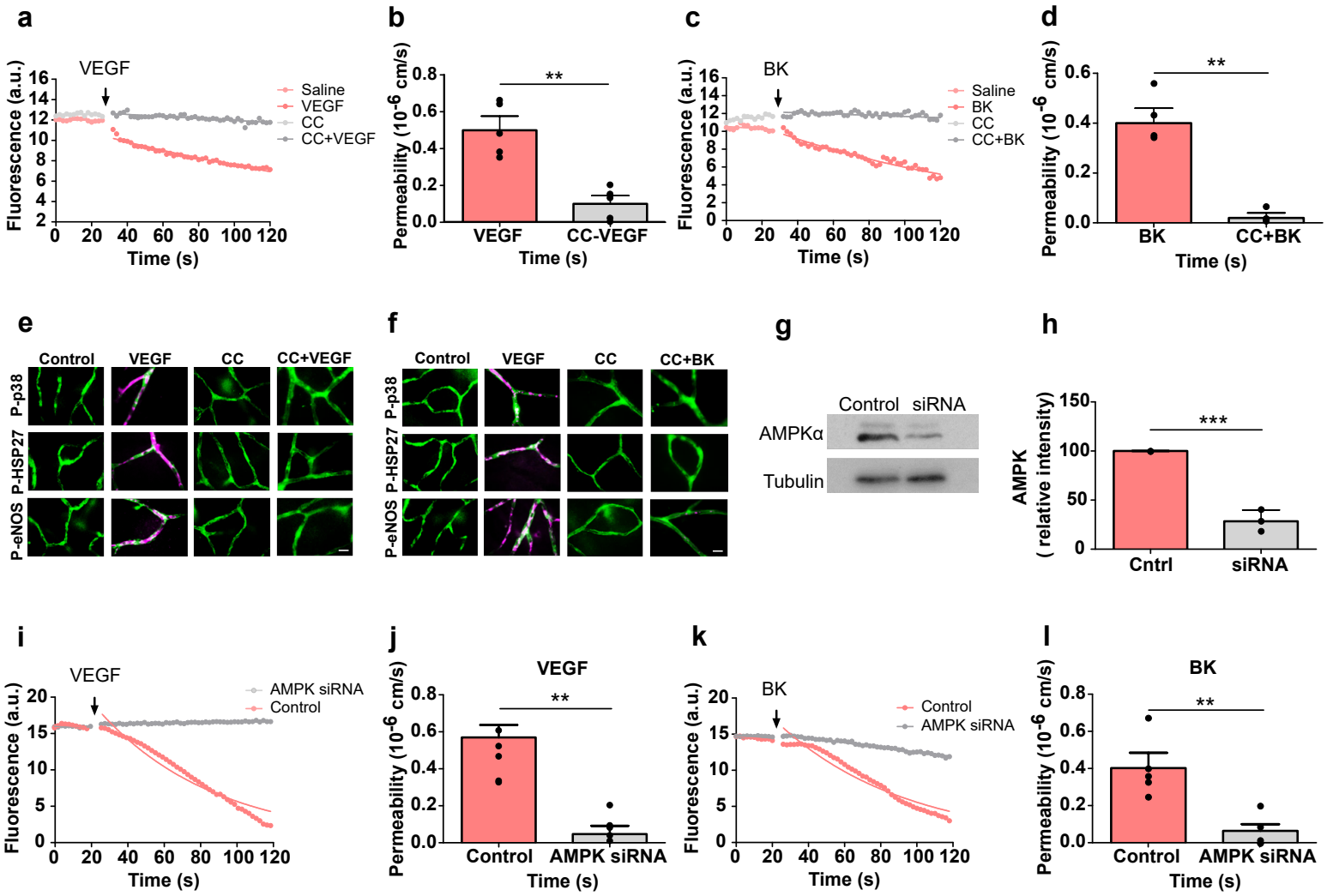

Figure 3. AMPK mediated VEGF-A/Bradykinin-induced permeability. (a-f) Mouse ex-vivo retinae were preincubated with or without Compound-C (10 μM) for 15 minutes. 10 ng/ml VEGF-A (a) or 10 μM BK (b) were then applied to the top of the retina and changes in fluorescence were recorded (c, d) or phosphorylation of p38, HSP27 and eNOS was assessed by staining (e, f). **(g-l)** AMPKα was knocked down by intravitreous injection of a specific siRNA (g, h) and ex-vivo retinae were isolated after at least 48h. VEGF-A (50 ng/ml) (I, k) or BK (10 μM) (j, l) did not induce any permeability in the knocked down ex-vivo retina. Representative results and quantifications (normalized mean ± SEM) from three independent experiments are shown. *$p < 0.05$, **$p < 0.01$, ***$p < 0.001$. Scale bars, 10 μm.

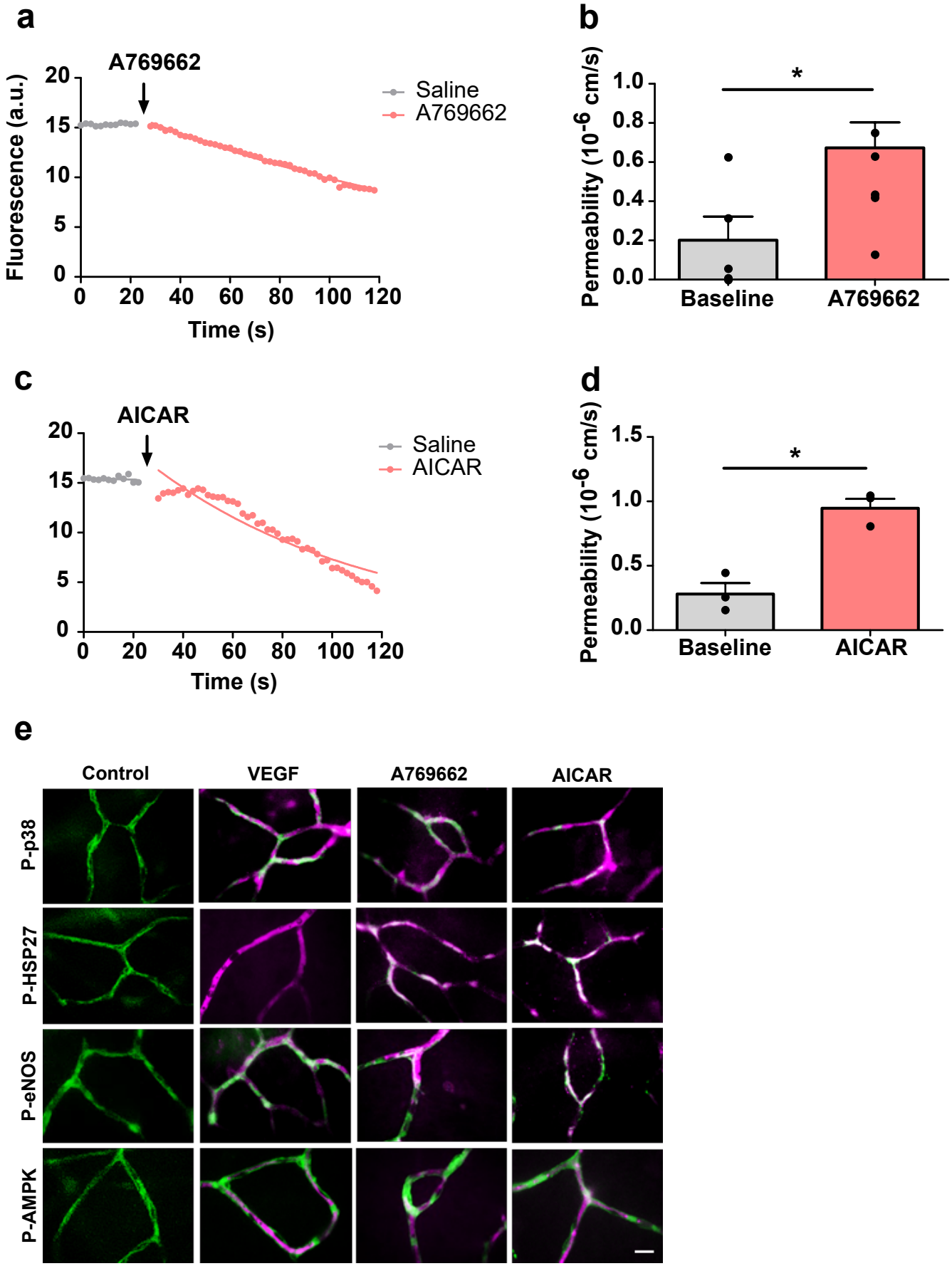

Figure 4. Stimulation of AMPK induced permeability in the ex-vivo retina. (a-e) Ex-vivo preparations were stimulated with two different AMPK activators named A769662 (10 μM) and AICAR (10 μM). Both agonists induced permeability in the ex-vivo retina (a-d) together with the activation of p38, HSP27 and eNOS (e). Permeability changes assembled from at least four retinae are shown.*$p < 0.05$, **$p < 0.01$, ***$p < 0.001$. Scale bars, 10 μm.

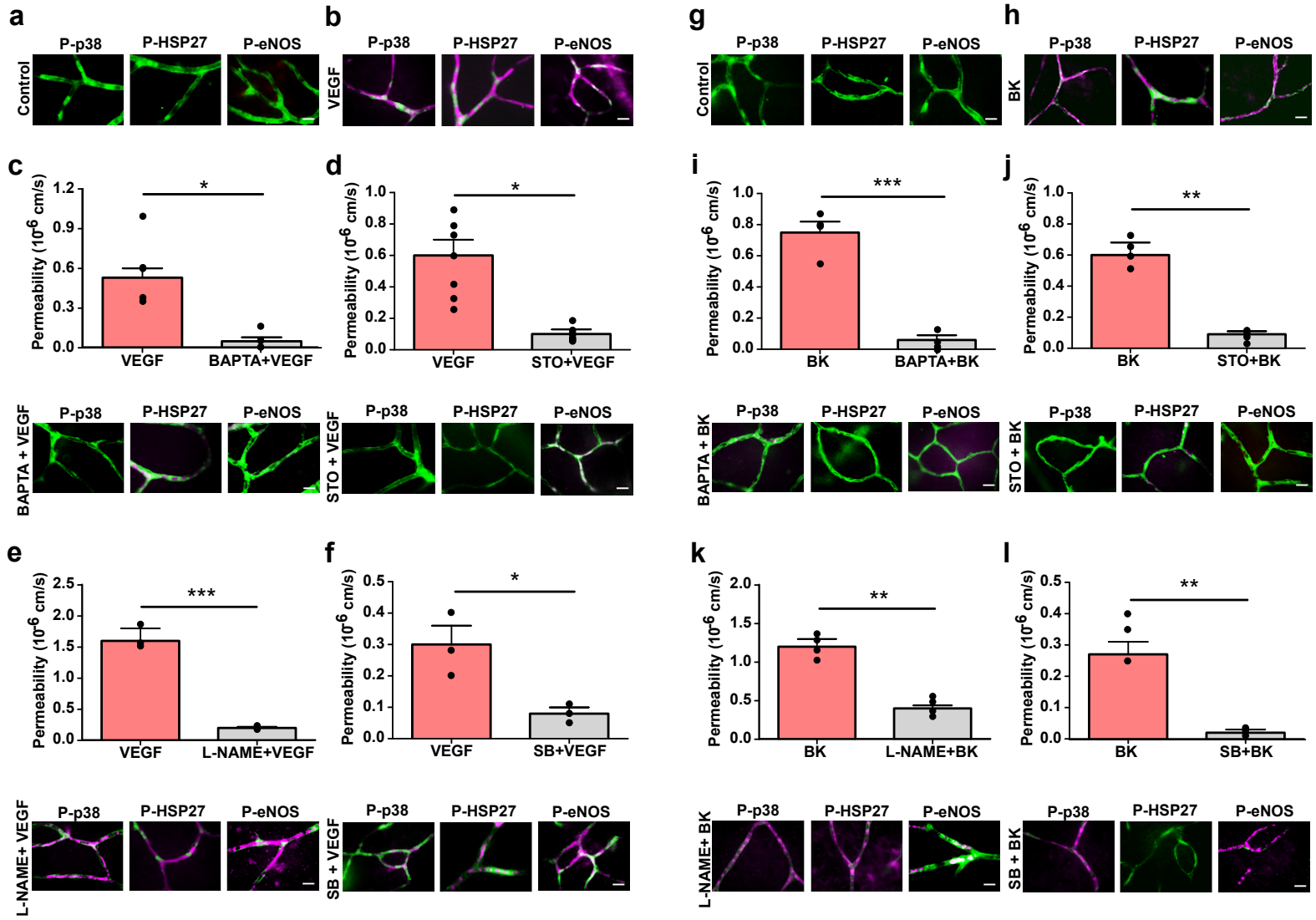

Figure 5. VEGF-A- and Bradykinin-induced permeability requires Ca2+ and activation of CaMKK, p38 and eNOS. (a-l) Ex-vivo retinae were preincubated with 20 μM BAPTA (Ca2+chelator) (c, i), or 10uM STO (CaMKK inhibitor) (d, j), or 10 μM L-NAME (eNOSinhibitor) (e, k) or 10 μM SB202190 (SB) (p38 inhibitor) (f, l), for 15 minutes and VEGF-A (50 ng/ml) or BK (10 μM) were then applied to the top of the retina (abluminal side) and changes in fluorescence were recorded or phosphorylation of p38, HSP27 and eNOS was assessed by staining. VEGF-A and BK-induced permeability was mediated by Ca2+, CaMKK, eNOS and p38. Representative results and quantifications (normalized mean ± SEM) from four independent experiments are shown. *$p < 0.05$, **$p < 0.01$, ***$p < 0.001$. Scale bars, 10μm.

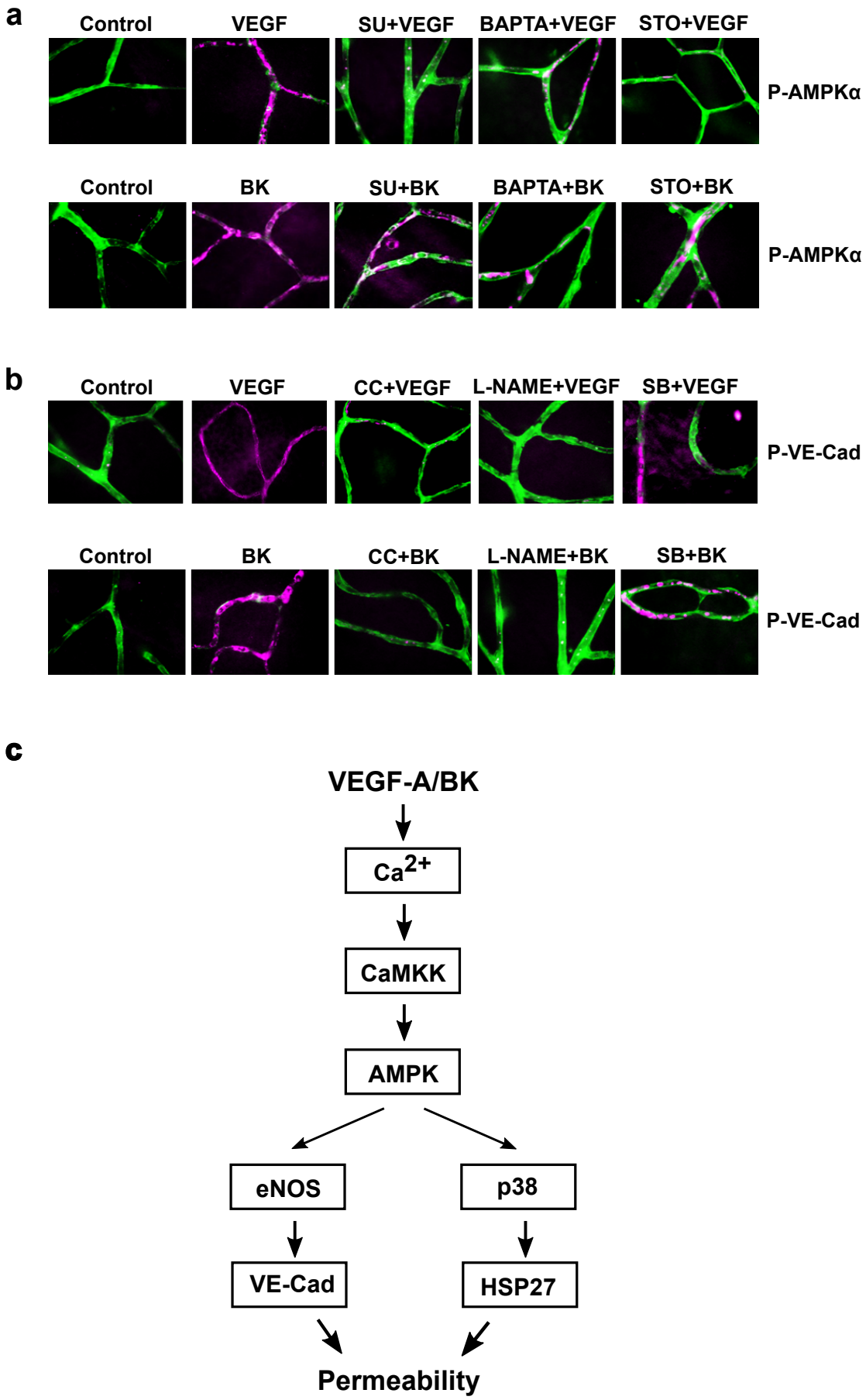

Figure 6. VEGF-A and Bradykinin induced VE-Cadherin phosphorylation
(a) Ex-vivo retinae were preincubated with SU1498 (10 μM), or BAPTA (20 μM) or STO (10 μM) and treated with VEGF-A and Brdykinin for 2 min. Retinae were then fixed with 4% PFA and whole mount stained for phospho-AMPKα (magenta) against IB4 (green). **(b)** Ex-vivo retinae were preincubated with compound C (10 μM), or L-NAME (10 μM) or SB202190 (10 μM), treated with VEGF-A and Bradykinin for 2 min and whole mount stained for phospho-VE-Cadherin (magenta) against IB4 (green). **(c)** Proposed signaling networks in the ex-vivo retinal microvasculature downstream of VEGF-A and Bradykinin. Scale bars, 10 μm.

Cannulation of the carotid artery and perfusion

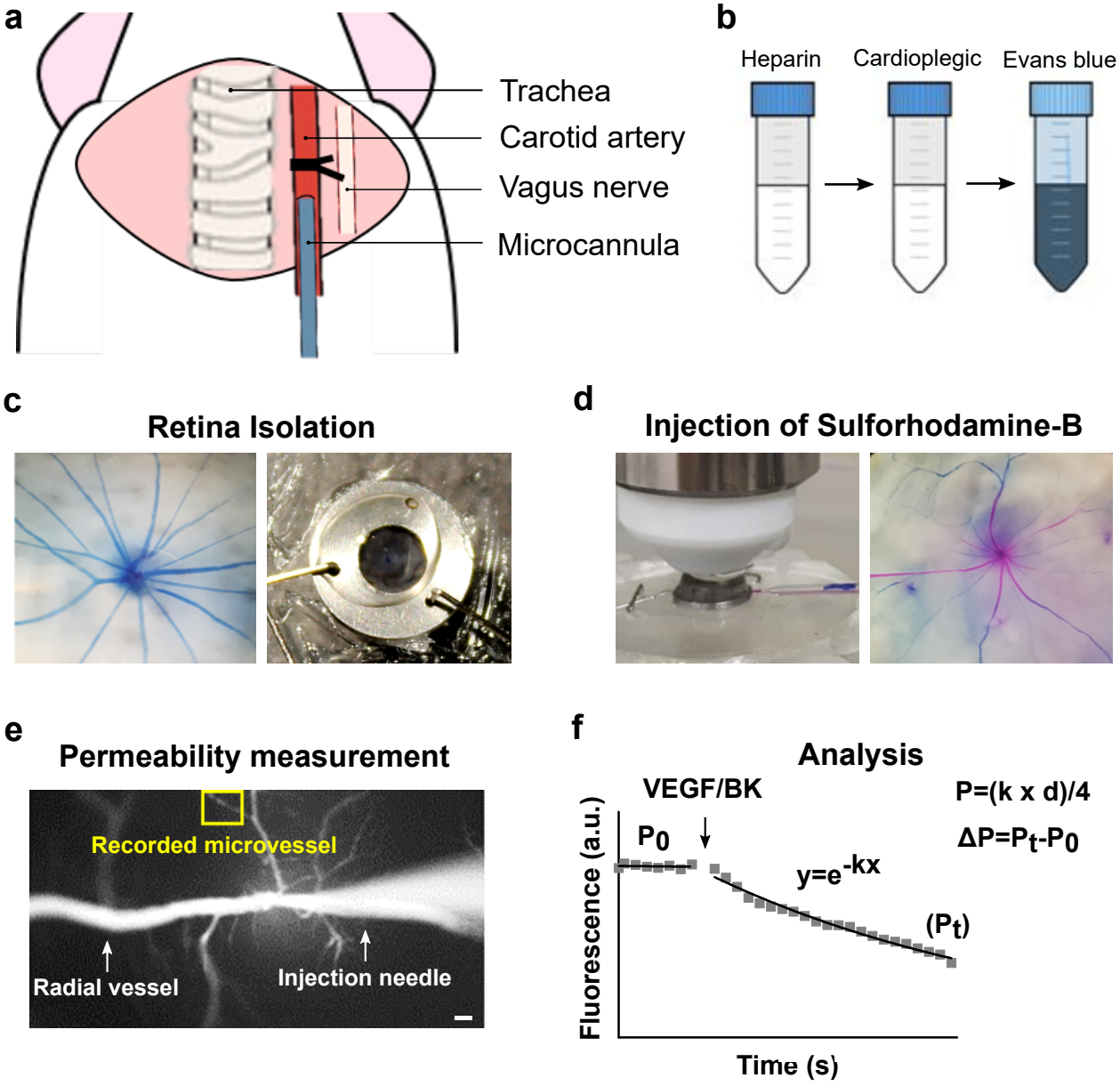

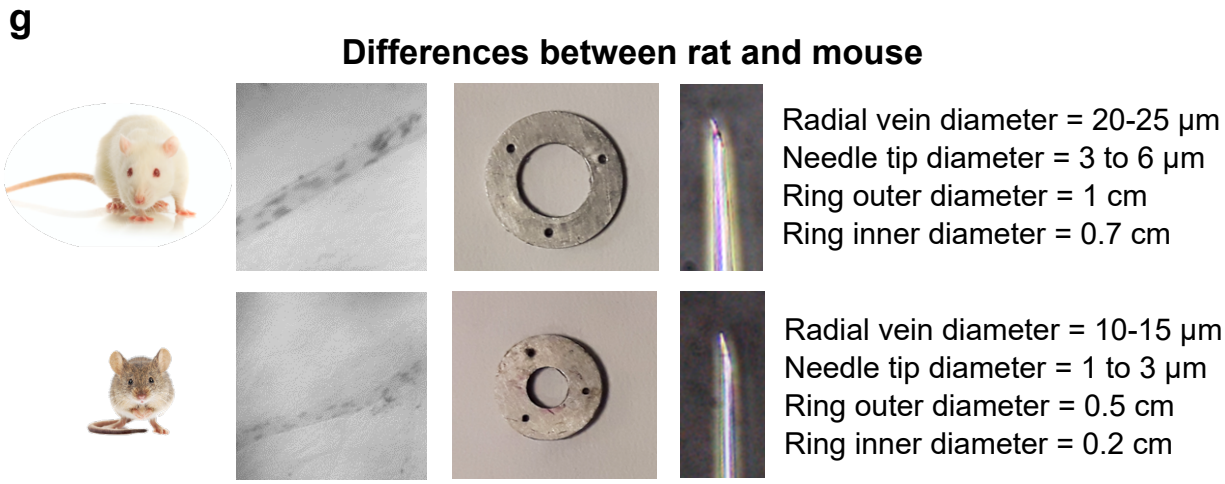

Supplemental Figure 1. The ex-vivo retinal model. (a-b) The carotid artery of a rat was separated from the surrounding tissues, cannulated using a microcannula (a) and consecutively perfused with heparin, cardioplegic solution without and with Evan's Blue (b). **(c-d)** The retina was isolated together with the sclera and flat-mounted onto a transparent silicon medium using a metal ring and pins (c). The retinal microvasculature was filled with Sulforhodamine-B through injection of a radial vessel using a sharpened glass capillary needle (d). **(e-f)** A capillary was chosen at least 200 µm away from the injection site (e) and the baseline fluorescence intensity within the vessel recorded for ca. 30 s before VEGF-A or BK were applied on top of the retina and permeability resulting in time-dependent loss of fluorescence (f). Scale bar, 20 µm. **(g)** Differences between the retinal vasculature and set-up in rats and mice. Shown are images of retinal microvessels, the metal mounting ring and the microinjection needles.

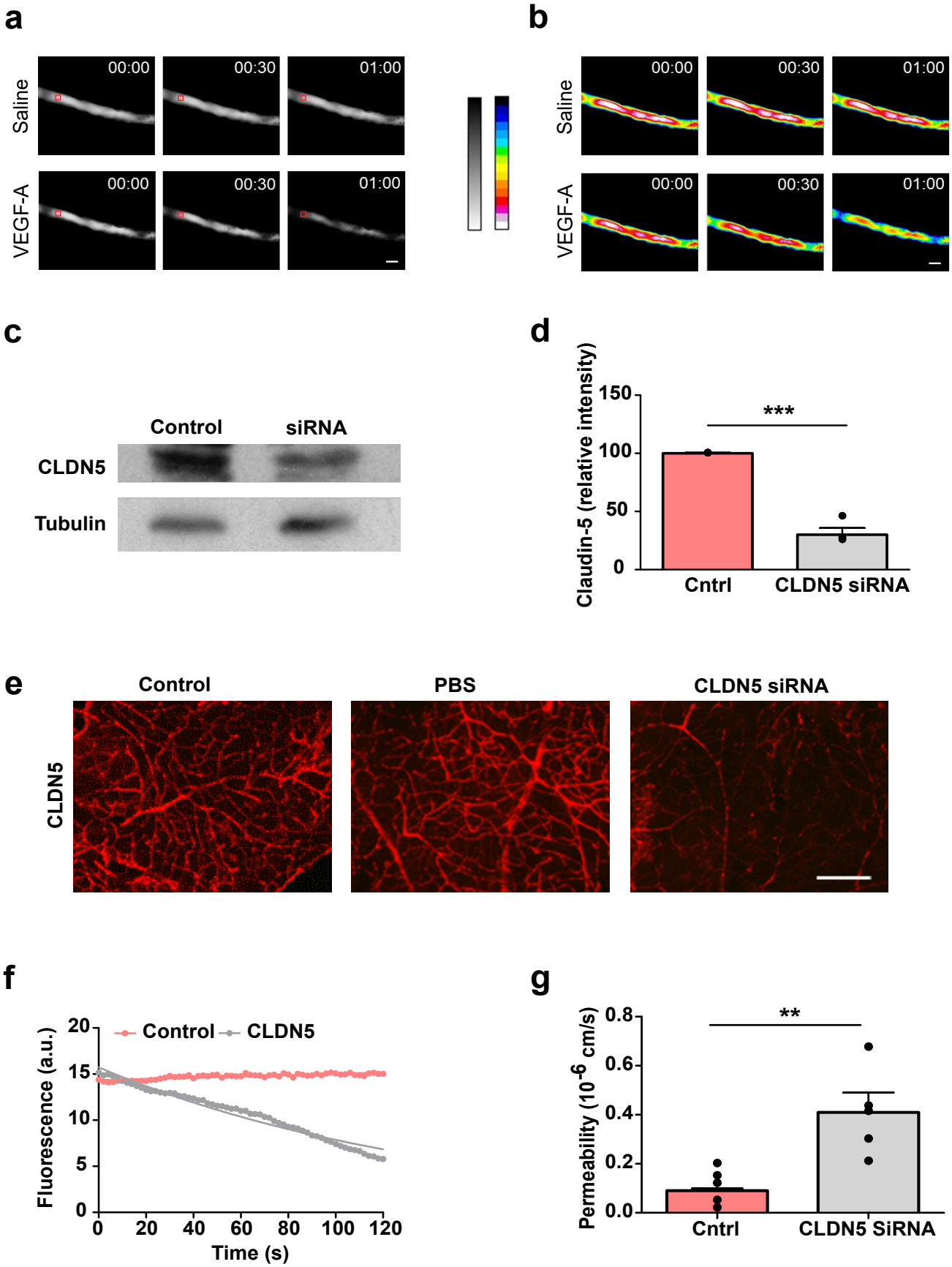

Supplemental Figure 2. Properties of the ex-vivo retina model. (a-b) Selected frames, pseudocoloured in (b), of timelapse measurement of a sulforhodamine-filled rat capillary before and after the addition of 50 ng/ml VEGF-A, illustrating the rapid loss of fluorophore from the lumen of the vessel. The red box indicates the r.o.i for intensity measurement. Scale bars, 10 µm. **(c-f)** CLDN5 siRNA was injected into mouse eyes. 48 h later CLDN5 levels were analysed by immunoblots of retinal lysates (c-d) or by wholemount immunochemical staining (e). Scale bar, 100 µm. Alternatively, permeability of 4 KDa Rhodamine was measured in ex vivo retinae from CLDN5 siRNA treated or control eyes (f-g). *$p < 0.05$, **$p < 0.01$, ***$p < 0.001$.